Influence of laser texturing on the wettability of PTFE

A. Riveiro (1,2), T. Abalde (1), P. Pou (1), R. Soto (1), J. del Val (1), R. Comesaña (2), A. Badaoui (2), M. Boutinguiza (1), J. Pou (1)

(1) Applied Physics Department, University of Vigo, EEI, Lagoas-Marcosende, Vigo, E36310, SPAIN

(2) Materials Eng., Applied Mech., and Construction Dpt., University of Vigo, EEI, Lagoas-Marcosende, Vigo, E36310, SPAIN

Abstract

Polytetrafluoroethylene (PTFE) is a synthetic fluoropolymer showing an excellent chemical resistance, high-temperature mechanical properties, high flexural strength or low friction coefficient. Due to its large stability, and hydrophobic nature, the wettability of PTFE surfaces can be reduced to transform them into superhydrophobic. In this regard, laser texturing is a fast, simple and versatile method to produce superhydrophobic PTFE surfaces in one-step, and over large areas. In this work, we used a CO_2 laser to modify the surface of PTFE samples. We studied the effect of the processing parameters (laser power or irradiance, scanning speed, and spacing -overlapping- between scan lines) on the wettability of textured surfaces using water, mineral oil and ethanol/water solutions as test fluids. Laser-treated surfaces showed a hierarchical micro- and nanotopography with a cotton-like appearance. The higher roughness and large quantity of air pockets make these laser-treated surfaces superhydrophobic, and highly oleophobic. Furthermore, they remain unaltered after being in contact with strong alkali and acid solutions or after slight friction. The self-cleaning performance of these surfaces was also demonstrated. The present findings suggest that CO_2 laser texturing of PTFE is suitable for the large-scale preparation of surfaces with a low-wettability to different liquids, with diverse applications in fields such as oil/water separation, self-cleaning surfaces, or in microfluidic devices.

Keywords

Polytetrafluoroethylene (PTFE); laser texturing; wettability; self-cleaning.

1. Introduction

Polytetrafluoroethylene (PTFE) is a synthetic fluoropolymer only composed by carbon and fluorine, and with multiple applications due to its excellent properties. The strong C-F bonds of fluoropolymers confer them with a large thermal stability, chemical inertness, low surface energy, electrical insulation, low friction coefficient, low dielectric constant, or an excellent charge storage stability [1-3]. These properties make it an excellent candidate to be applied in fields such as electrical, mechanical, textile, biomedical, pharmaceutical or food, among others [4]. The wettability of PTFE surfaces has been researched in the past to expand their current applications. In this sense, the low wettability of PTFE hinders its application in the biomedical field; then, different surface treatments (e.g. laser or plasma treatments) have been tested to improve its wettability and to promote the cell adhesion, and proliferation of PTFE-based implants [5, 6]. On the contrary, the low wettability of PTFE surfaces can be even more reduced to obtain superhydrophobic surfaces [7, 8]. These low-wetting surfaces are extremely interesting for many applications, such as in drag reduction, self-cleaning or anti-icing surfaces [9-12]. Different techniques or physical/chemical procedures have been applied to obtain this kind of surfaces, such as plasma treatment, abrasion with sandpapers, laser treatments or deposition of colloidal coatings [12-15]. Among these techniques, laser texturing is one of the most versatile and efficient processes to tailor the surface properties of metals, ceramics and polymers, in particular, to modify the wettability of PTFE surfaces [16-19].

Laser texturing involves the utilization of a focused laser beam, which heats, melts, and/or vaporizes the surface of the polymer to produce regular or irregular patterns of bumps, dimples, or grooves [20, 21]. These patterns modify the roughness of the surface, and then, its apparent wettability due to the formation of air pockets in the surface. On the other hand, the utilization of UV lasers (e.g. excimer lasers) can also produce the breaking of chemical bonds in the surface; this can induce the formation of functional groups, and then the modification of the surface chemistry of the polymers [18]. These modifications will also impact on the apparent wettability of the surface.

In the literature, many different works have explored the utilization of laser texturing to modify the surface roughness or the surface chemistry of the PTFE surfaces. The utilization of femtosecond lasers to modify the surface topography of PTFE has been largely explored in different research works. In this way, Huang et al used a femtosecond laser (λ=800 nm) to treat PTFE surfaces. The micro- and nanostructures formed after laser texturing turned the PTFE

surfaces into superhydrophobic [22]. Kietzig et al and Liang et al found that these nanostructures consisted of a hairy-like structure, where a forest of entangled fibers supported the structural superhydrophobicity [23, 24]. It was showed that this micro- and nanostructure changed with the accumulated laser fluence. Moreover, these surfaces showed applications for anti-adhesive and anti-wetting applications. Li et al also found that these surfaces could be suitable for oil/water separation due to the inverse superhydrophobicity and superoleophilicity showed by the laser-treated PTFE surfaces [25]. Toosi et al determined the influence of the laser processing parameters (fluence, scanning speed, and beam overlapping) during laser texturing of PTFE surfaces with a Ti:Sapphire femtosecond laser (λ=800 nm) [26]. Superhydrophobic surfaces were also produced. Similarly, Fan et al. used a Ti:Sapphire femtosecond laser (λ=800 nm) to produce a groove-like microstructure on PTFE samples [27]. In this case, the influence of the microtopography on the wetting was analysed, and superhydrophobic and superoleophobic surfaces were obtained. Moreover, the impact of the distance between microgrooves on the apparent wettability of the PTFE surfaces was determined. Yoo et al showed that these micro- and nanotopographies produced on PTFE by laser texturing with a femtosecond laser (λ=400 nm) are also suitable to be transferred to a PDMS surface [28]. This surface also shows superhydrophobic properties.

Other research works explored the utilization of UV lasers to modify the surface topography but also the surface chemistry of PTFE surfaces. Gotoh et al showed that the wettability of PTFE surfaces irradiated with a Xe_2 excimer laser (λ=172 nm) is not substantially modified for processing conditions not involving topographical changes [29]. However, other research works showed that the wettability is modified if the process is performed in a suitable solution. In this way, Hopp et al used an ArF excimer laser (λ=193 nm) to change the surface energy of PTFE samples and improve their adhesion properties [30]. This treatment showed the increment of the adhesion of treated surfaces only when performed in the presence of 1,2-diaminoethane photoreagent. Inazaki et al also showed a similar behavior when the laser treatment, using an ArF excimer laser (λ=193 nm), is performed in the presence of monosodium L-glutamate monohydrate (L-Glutamate) or in ethyl alcohol solutions [31]. In both cases, the laser treated surfaces evolved to a hydrophilic state due to the reduction of fluorine in the surface and the formation of amino and carbonyl groups and ethylene linkages. Other works using UV laser radiation (but not produced with excimer lasers) showed more intense changes in the wettability of the treated areas. In these cases, the modification of the wetting properties relies in the change of the surface topography (as in the case of the treatment with femtosecond lasers) instead of in the surface chemistry. In this way, Qin et al used a picosecond UV laser

(λ=355 nm) to produce micro- and nanostructured surfaces with superhydrophobic properties [32]. The modification of the spacing between scan lines was determined as the most relevant parameter to tune the water adhesion of the treated surfaces. Similarly, Žemaitis et al also used a picosecond UV laser (λ=355 nm) to produce riblet surfaces in PTFE samples [33]. These surfaces also showed a potential application for drag reduction.

Despite this intensive research into the laser texturing of PTFE surfaces, the utilization of CO_2 lasers is quite restricted. CO_2 lasers offer many advantages as compared to the processing with femtosecond and excimer lasers. These laser sources are very reliable, more efficient, commonly used in the industry, not requiring complex experimental setups (e.g. vacuum chambers), and in general, cheaper. In this regard, Waugh et al demonstrated the reduction of wettability in PTFE surfaces after CO_2 laser texturing [34]. These surfaces showed a higher osteoblast cell and stem cell growth suitable for biomedical applications. Similarly, Zhan et al showed that these surfaces exhibit a self-cleaning and anti-icing behavior [9]. However, the influence of the processing parameters or the wetting properties with test fluids other than water has not yet been explored.

In the present work, we investigated the CO_2 laser texturing of PTFE surfaces. The influence of the processing parameters (laser power or irradiance, scanning speed, and spacing -overlapping- between scan lines) on the wettability of laser-treated PTFE surfaces using four different test fluids (water, mineral oil, water 60% + ethanol 40% and water 80% + ethanol 20%) is studied. Furthermore, we have explored the potential utilization of these laser-treated PTFE surfaces for self-cleaning applications.

2. Materials and methods

2.1. Materials

The present study was carried out on flat samples of polytetrafluoroethylene (PTFE). This polymer is a thermoplastic material with multiple carbon–fluorine bonds. It shows a high strength, toughness, good flexibility, and a low friction coefficient. It is resistant to a large range of chemicals (solvents, acids and bases), and has an excellent corrosion resistance to almost all chemicals. Sheets of 80 mm x 80 mm x 1.5 mm with an average surface roughness of R_a= 0.64 µm were used in the experiments.

After the laser treatment, the surface of the samples was cleaned by ultrasonic treatment in deionized water during 5 minutes.

2.2. Experimental procedures

The experiments were performed using a CO_2 laser source (Rofin-Sinar SMG 025 A) emitting a TEM_{00} laser beam at a wavelength of 10600 nm. The laser beam was focused on the surface of the PTFE samples using a flat field lens, 300 mm in focal length. In this case, the laser spot diameter on the surface of the samples was around 300 µm. Galvanometric mirrors were used to scan the laser beam across the polymeric samples. In all the cases, the treatments were performed in air and at atmospheric pressure.

The processing parameters evaluated during the experiments include the laser power (W) (or the irradiance, W/mm^2), scanning speed (mm/s) and the spacing between scan lines (mm). The spacing between scan lines is considered between the centers of the engraved lines; therefore, an overlapping between adjacent scan lines is observed. The value for the overlapping between scan lines (ranging from 20 to 90%) is also included in Table 1. The range of values for these processing parameters is summarized in Table 1.

Table 1. Processing parameters evaluated during the experimental tests.

Laser power P (W)	12.5, 15, 17.5, 20.5, 22.5
Irradiance I (W/mm^2)	122.8, 147.4, 171.9, 201.4, 221.0
Scanning speed v (mm/s)	150, 275, 400
Spacing between scan lines Δx (mm)	0.031 (90%), 0.0625 (80%), 0.125
(or overlapping in %)	(60%), 0.250 (20%)

2.3. Sample characterization

Selected samples were inspected in frontal view to the laser treated area using an optical microscope (Nikon SMZ-10A) and a FE-SEM microscope (JEOL JSM-6700 f) after surface metallization with gold.

ATR-FTIR measurements of the as received, and laser-treated PTFE samples were carried out using an ATR-FTIR spectrometer (Cary 630, Agilent) to determine possible chemical surface modifications.

Average roughness (R_a) was measured using a Veeco Dektak 3ST surface profiler in several locations of the treated areas; then, an average value was extracted. Measurements were made in accordance with the recommendations specified in the International Standard ISO 4288:1996.

Wettability at room temperature was determined using a goniometer measuring system (Ossila Ltd) and with deionized water, mineral oil (Hyspin AWS 46, Castrol), and two water/ethanol mixtures (water 60%v/v + ethanol 40%v/v, and water 80%v/v + ethanol 20%v/v) as test fluids. Contact angle measurements (CA) were performed using the sessile drop method. ~ 5 µl drops of each test fluid were deposited on the samples with a micropipette, following the recommendations given by the European standard EN 828:2013. The sliding angle, and contact angle hysteresis (CAH) was also determined for each test fluid by using the tilting plate method. The stability of CA values for the laser-textured surfaces was confirmed by measurements after 150 days elapsed from the processing. Averages and standard deviation of three independent measurements were registered for each sample and characterized angle.

3. Results and discussion

3.1. Surface topography characterization

Optical micrographs of the laser-treated PTFE surfaces are depicted in Fig. 1. As observed, a cotton or spongy-like structure, showing a large micro- and nanoporosity, is produced after the laser treatment. This spongy-like structure is more pronounced for lower scanning speeds, as observed in Fig. 1b. In this case, the micro-channels are not so evident, and a spongy-like structure, more uniformly distributed, is formed. A detailed view of the treated areas, obtained by FESEM (see Fig. 2), reveals that this porous structure contains a large amount of fibers fused together. The formation of this fiber structure is responsible for the large quantity of air pockets in the treated surfaces, which will have a substantial impact on the wettability of the treated areas.

PTFE shows a large absorption to the CO_2 laser radiation, evolving the absorptivity from 67% at ambient temperature (27.5 ºC), up to 98% at 300 ºC, as reported by Tarasenko et al [35]. This leads to a fast increase in the temperature, reaching up to 1300 ºK, as reported in [36] (for similar processing conditions), and to the ablation of a groove. Two main ablation products are produced in these grooves: (1) a gas flow produced by the decomposition of the polymer, and (2) streams of melt drawn into fibers. The gaseous decomposition products were determined to be tetrafluoroethylene monomers and fluorocarbons, as reported by Tosltopytov [36]. The elongation of the streams of molten material produces fibers which are fused together to form

this spongy-like structure. The process of elongation is hypothesized to be due a consequence of the action of the gaseous decomposition products which elongate the melt along the flow, or due to the action of the vaporization-induced recoil force, i.e. the recoil momentum induced on the melt by the intensive evaporation produced in the irradiated surface [37]. Both mechanisms depend on the temperature of the melt as the higher the temperature, the higher the amount of gaseous decomposition products and also the recoil forces [37], and then, the ability to elongate the melt. This process of elongation will be also dependent on the viscosity of the melt, which is also inversely proportional with the temperature of the melt. The higher the temperature, the lower the viscosity, and the easier the drawing of the melt into fibers [38]. It should be pointed out that the temperature in the irradiated area is directly related to the processing parameters, especially, laser power and scanning speed as both determine the amount of energy deposited in the surface per unit of length. The higher the deposited energy, the higher the temperature reached by the melt. The spacing between scan lines (i.e. overlapping), has an impact on the temperature, but the main effect of this processing parameter is that for a low spacing (i.e. higher overlapping) a larger extension is treated, and a denser spongy structure is formed.

The proposed mechanism for the formation of the fibers agrees with that proposed by Tosltopytov et al [39], although, in this work, the influence of the recoil pressure is not considered.

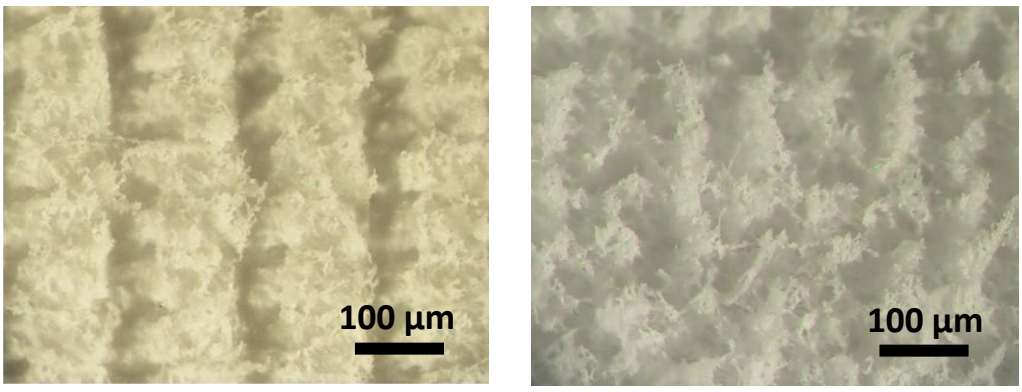

Figure 1. Optical micrographs showing the surface of laser-treated PTFE samples with a scanning speed of: a) v=275 mm/s, and b) v=150 mm/s. (Processing conditions: P=17.5 W, Δx=0.150 mm).

The influence of the processing parameters on the average roughness of the laser-treated PTFE surfaces is depicted in Fig. 3. As noticed, the spacing between scan lines is the most relevant

parameter (for the range of tested values) affecting the final roughness. The shorter the spacing, the higher the average roughness. The highest value of average roughness, around $R_a \approx 35$ µm, is obtained for a spacing of $\Delta x = 0.031$ mm. On the other hand, the laser power (or irradiance) increases the average roughness; however, this increment is smaller as compared to that found for the spacing between scan lines. The influence of the scanning speed is more complex. The average roughness increases with the scanning speed up to a maximum value where the average roughness decreases. This maximum appears for a scanning speed around $v \approx 275$mm/s (see Figs. 3b,c).

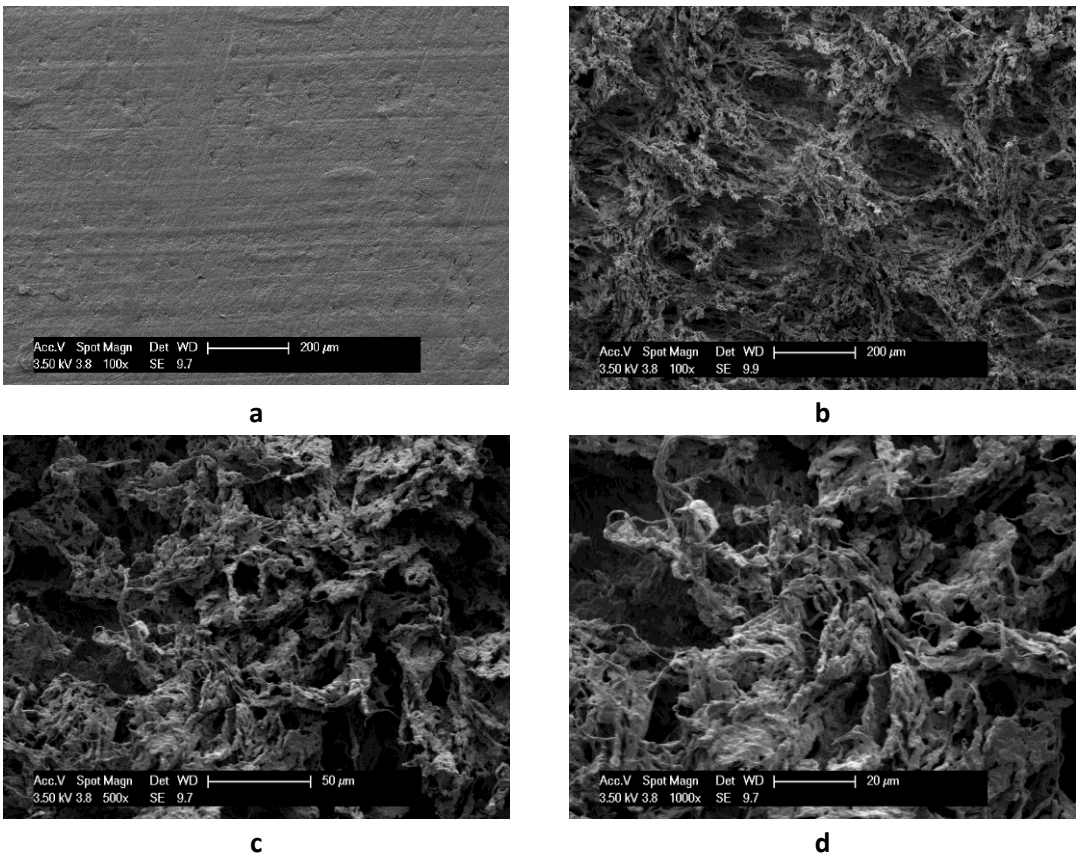

Figure 2. SEM micrographs showing the surface of the a) pristine and laser-treated PTFE samples at b) 100x, c) 500x and d) 1000x magnifications. (Processing conditions: P=17.5 W, v=150 mm/s, Δx=0.125 mm).

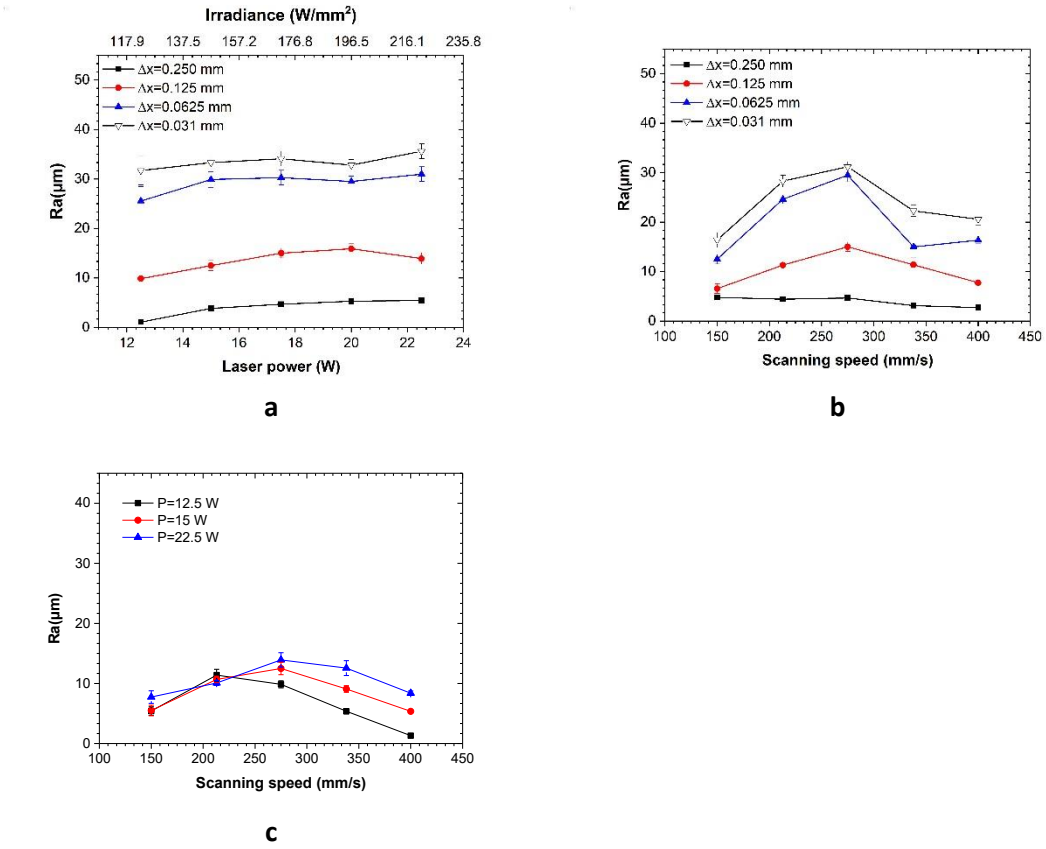

Figure 3. Variation of the average roughness R_a (μm) with: a) the laser power for four spacing between scan lines (Processing conditions: v=275 mm/s), b) scanning speed for four spacing between scan lines (Processing conditions: P=17.5 W), and c) scanning speed for three different laser powers (Processing conditions: Δx=0.125 mm).

The influence of the processing parameters on the roughness can be explained in terms of the energy (per unit of length or area, if one or several scan lines, respectively, are considered) deposited on the surface. The increment of the laser power produces a higher roughness as a consequence of the higher ablation due to the larger energy per unit of length deposited on the surface, as seen in Fig. 3a. Higher temperatures are reached in a grooved line. Furthermore, more melt with a lower viscosity is produced, and this is more easily drawn into fibers. Notice that the variation of the roughness with the laser power tends to be less pronounce as the spacing between scan lines is reduced (due to the interaction of the laser power with the spacing as discussed below).

Similarly, the reduction of the spacing between scan lines (i.e. a higher overlapping) for a constant laser power is able to deposit a larger amount of energy per unit of area. Then, a larger surface is ablated, and the temperature of the melt is higher leading to a higher roughness as before, as seen in Fig. 3a. However, the increment of the roughness with the spacing is less

pronounced for values of Δx=0.031 mm and 0.0625 mm, as observed in Figs 3a and 3b. This is a consequence of the large overlapping between scan lines (80% and 90%, respectively) and the destruction of the topography created in one groove by the subsequent ones.

On the contrary, the scanning speed reduces the amount of energy per unit of length in one scan line. Then, the ablation of the surface is reduced, and less molten material is produced. Therefore, a reduction of the roughness with the scanning speed is expected. However, this trend is only observed in Fig. 3b for a spacing between scan lines of Δx=0.250 mm, when the overlapping between scan lines is quite low (20%). For a smaller spacing (Δx=0.031, 0.0625, and 0.125 mm), the roughness increases with the scanning speed, and it is only reduced from a scanning speed of v≈275 mm/s. This contradictory trend is explained due to the interaction between the scanning speed and the spacing between scan lines. For a low spacing between scan lines and a low scanning speed, the overlapping between scan lines (grooves) is large (between 60% and 90%), and the energy per unit of area is excessive. The adjacent scan lines tend to destroy the previously ablated areas and the filaments drawn from the melt tend to fuse together easier, then, leading to a more uniform and less rough surface. As the scanning speed is increased from a value of v=275 mm/s, this effect tends to be minimized, and scanned lines are less affected by the subsequent ones. This effect can be guessed in Fig 1 (grooves are easily identified for a scanning speed of v=275 mm/s, while for v=150 mm/s they are less clearly observed). A similar explanation can be applied to the interaction between laser power and scanning speed shown in Fig. 3c. For a low scanning speed, the energy deposited per unit of length is excessive, and one scan line tends to destroy the topography developed in the prior scan line. The increment of the scanning speed tends to minimize this effect and the roughness is only slightly increased up to a scanning speed of v=275 mm/s. A further increment of the scanning speed minimizes this interaction, as the energy per unit of length in the groove is substantially reduced, and the roughness decreases.

3.2. Surface chemistry characterization

FTIR analyses of the pristine and laser-treated surfaces were undertaken to elucidate a possible chemical modification of the PTFE surfaces after the laser treatment (see Fig. 4). At high wavenumbers, peaks at 1198 cm^{-1}, and 1142 cm^{-1} are observed. They correspond to CF_2 stretching. At lower wavenumbers, the peak at 639 cm^{-1} corresponds to C-C-F bending, while at 553 cm^{-1}, and 505 cm^{-1} correspond to CF_2 bending [40]. These spectra do not show relevant chemical modifications in the surface after the laser processing, irrespectively of the processing parameters.

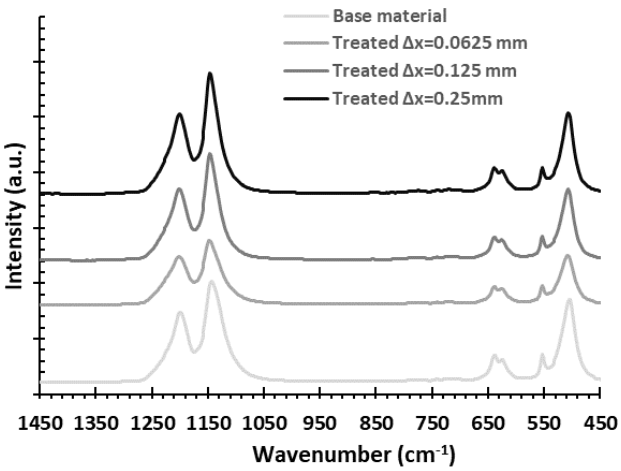

Figure 4. ATR-FTIR spectra of the pristine and laser-treated PTFE surfaces for three different spacing between scan lines: Δx=0.0625, 0.125 and 0.25 mm. (Processing conditions: P=17.5 W, v=150 mm/s).

3.3. Wettability characterization

We investigated the influence of the processing parameters on the wettability of the laser-treated surfaces for four different test fluids: water, mineral oil, and two mixtures of water and ethanol (Water 60%+EtOH 40%, and Water 80%+EtOH 20%). As depicted in Fig. 5a, the higher the laser power, the lower the wettability of the laser-treated surfaces (and higher contact angles are observed) irrespectively of the liquid used in the experiments. This increment of the contact angle is a direct consequence of the higher roughness obtained with the increased laser power (or irradiance), as chemical modifications in the surface were not observed. This result can be interpreted using the Cassie-Baxter equation [41]. According to this equation, the apparent contact angle θ_c for a liquid droplet in a rough surface is given by:

$$\cos\theta_c = f_1 \cos\theta_1 - f_2 \quad \text{with} \quad f_1 + f_2 \geq 1 \tag{1}$$

where f_1 is the total area of PTFE under the droplet per unit projected area under the droplet, θ_1 the contact angle on a smooth PTFE surface, and f_2 the total area of air under the droplet per unit projected area under the droplet (notice that we should not use the Cassie-Baxter equation, commonly expressed as $\cos\theta_c = f\cos\theta_1 - (1-f)$, as this would require of coplanar liquid-vapor and solid-liquid interfaces, which is not the case [41]). In a simplified way, the increment of the roughness increases the amount of air pockets; then, the fraction f_2 increases, and the apparent contact angle θ_c too. This explains the increment of the contact angle with the laser power (or irradiance), as the roughness is increased with the laser power (see section 3.1).

The increment of the contact angle with the laser power (Fig. 5a) is less pronounced for water than for the rest of liquids due to the hydrophobic nature of the base material. The maximum contact angles are obtained for a laser power of 22.5 W (spacing between scan lines Δx=0.250 mm), and they have a value around CA≈135° for water, and CA≈123° for the rest of liquids. On the other hand, the scanning speed has a contrary effect (Fig. 5b): the higher the scanning the speed, the lower the roughness (see section 3.1), and the higher the wettability (and then, lower contact angles are observed). This reduction of the contact angle is also less pronounced for water, going from a CA≈135° to 116°. Therefore, it can be concluded that the CO_2 laser processing of PTFE surfaces can easily produce highly hydrophobic (or even superhydrophobic) surfaces, irrespectively of the processing parameters.

The influence of the laser power and spacing between scan lines for each test fluid was also determined. As noticed in Fig. 6, the contact angle for the water droplets deposited in the laser-treated PTFE surfaces is larger than for the rest of test fluids. In this case, the contact angle is always in an interval of 120-135°, and irrespectively of the processing conditions. For a spacing of equal or less than Δx=0.125 mm the contact angle does not vary in excess with the laser power as there is a large overlapping between scan lines, and roughness does not significantly increase (see section 3.1); however, for a larger spacing (Δx=0.250 mm), the overlapping decreases, and the roughness is more affected by the laser power (see section 3.1). In consequence, the contact angle slightly increases with the laser power.

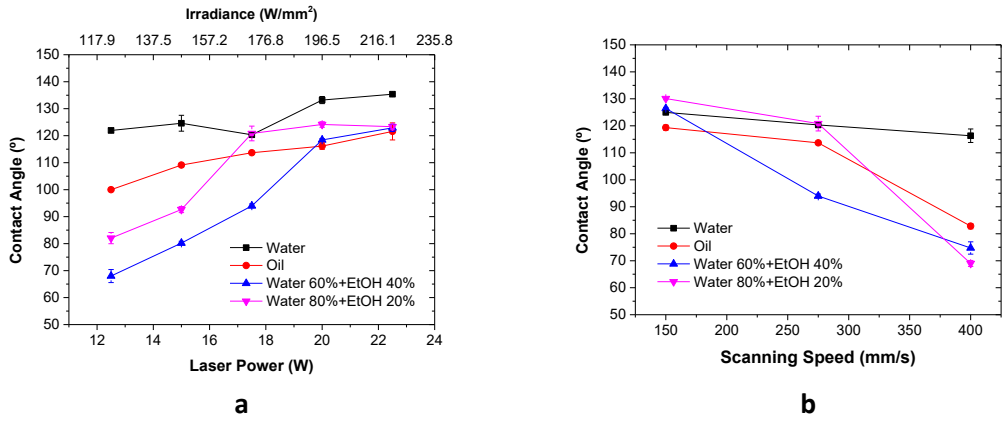

Figure 5. Influence of the laser power (Processing conditions: Δx=0.250 mm, v=275 mm/s) and scanning speed (Processing conditions: P=17.5 W, Δx=0.250 mm) on the contact angle using: water, oil, Water 60%+EtOH 40%, Water 80%+EtOH 20% as test fluids.

When using oil as test fluid, the contact angle is in a range of 100-126°. In this case, the observed trend is similar to the case of using water. For a spacing lower than Δx=0.250 mm, the value of the contact angle is almost constant with the laser power; however, for a spacing of Δx=0.250 mm, the contact angle slightly increases with the laser power.

For the ethanol/water mixtures, i.e. water 60% + ethanol 40% and water 80 % + ethanol 20% mixtures, the contact angles are in the ranges 68-120° and 82-126°, respectively. The contact angle is slightly higher for the mixture with higher content of water (i.e. for water 80 % + ethanol 20%). On the other hand, the contact angle significantly increases with the laser power for a spacing of Δx=0.250 mm, while for a lower spacing this remains almost constant. This increment is more relevant for the mixture with a lower water content (i.e. for water 60% + ethanol 40%).

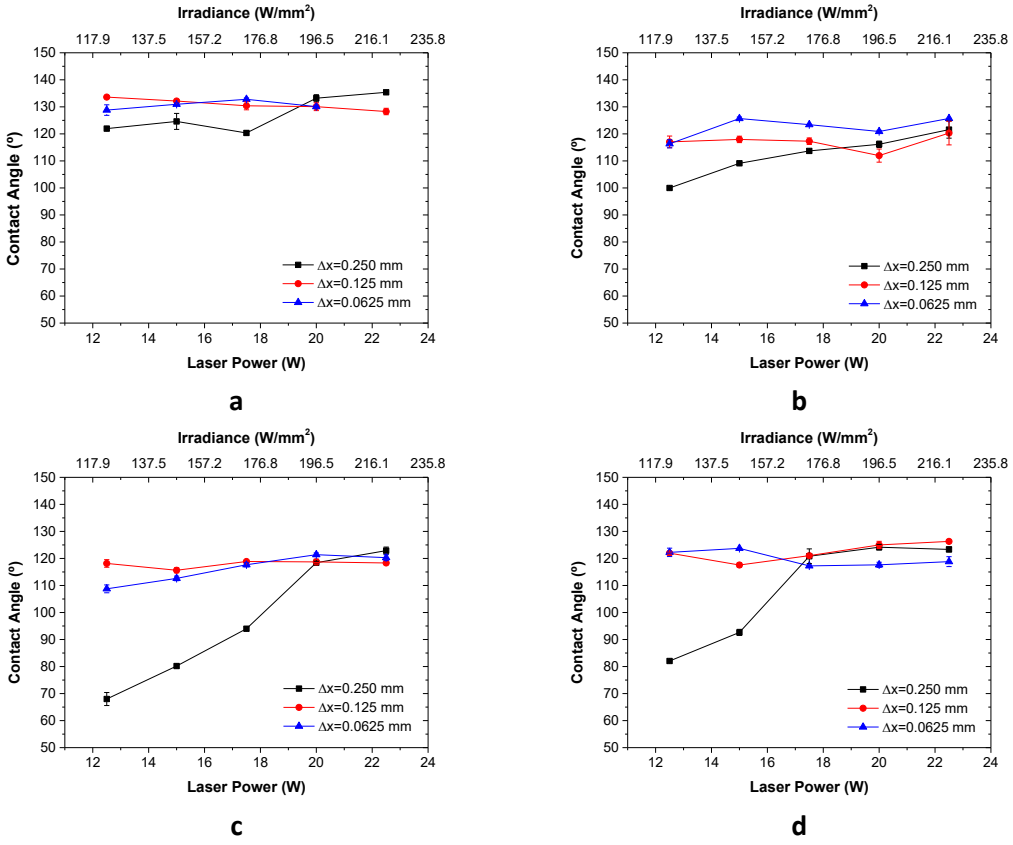

Figure 6. Influence of the laser power on the contact angle for different spacing of scan lines using: a) water, b) oil, c) Water 60%+EtOH 40%, d) Water 80%+EtOH 20% as test fluid. (Processing conditions: v=275 mm/s).

The measurement of the sliding angle reveals that this parameter is lower when using water as test fluid (see Fig. 7). A sliding angle of ≈5° (common in superhydrophobic surfaces) is observed

for water, while for oil, water 60%+ethanol 40%, and water 80%+ethanol 20% are ≈30°, ≈12°, and ≈12° respectively. On the other hand, the laser textured surfaces show low contact angle hysteresis (CAH≈3°) when water is used as test fluid. For the rest of fluids, the hysteresis is considerably higher, especially for oil (CAH≈40°). These higher values are related to a superior adhesion of these fluids to the treated surface, as pointed out by Xiu et al. [42]. This result is in agreement with the higher sliding angles observed for these test fluids.

The analysis of the previous results suggested us the suitable processing conditions required to obtain low wetting surfaces, i.e. highly amphiphobic PTFE surfaces. In this sense, a laser power P>20W, a scanning speed v<275 mm/s, and a spacing between scan lines Δx<0.125 mm are required to produce such surfaces, as shown in Fig. 8. As observed in these images, surfaces with a superhydrophobic nature are produced. Furthermore, they are also highly oleophobic and the wettability to mixtures of water and ethanol is also largely reduced. For these last test fluids, the increment of the contact angle is quite large, around 60% after the laser processing.

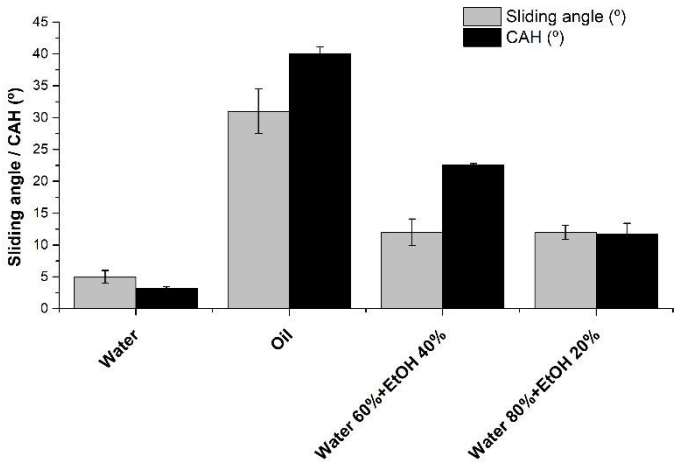

Figure 7. Sliding angle and contact angle hysteresis (CAH) as a function of the test fluid. (Processing conditions: P=17.5 W, v=150 mm/s, Δx=0.250 mm).

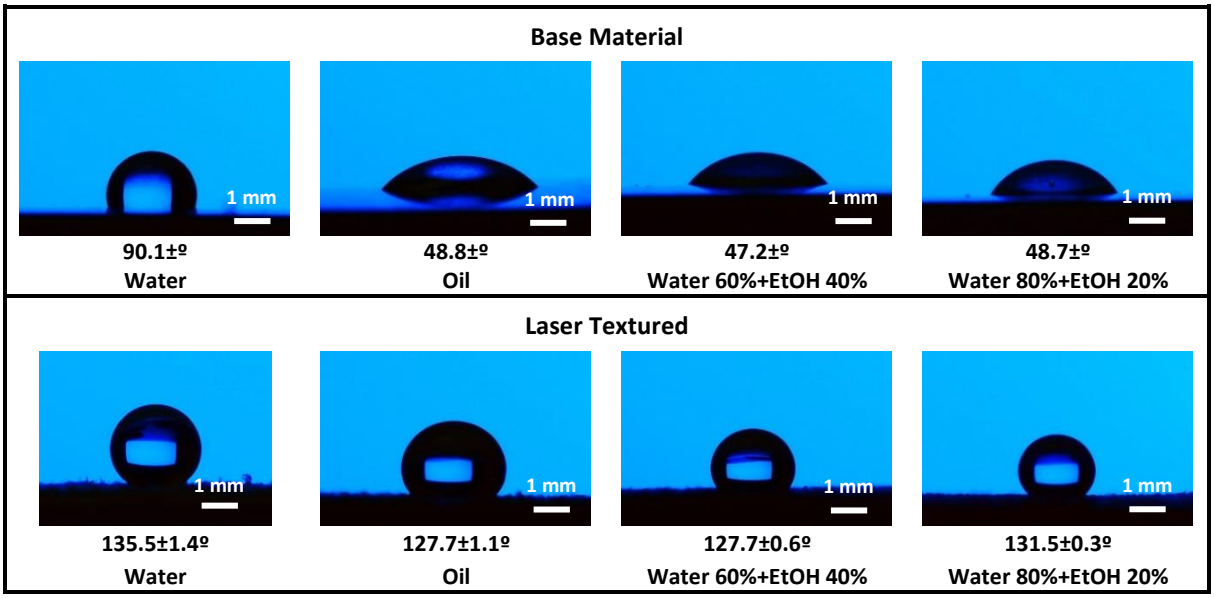

Figure 8. Maximum contact angles for the untreated and laser-treated PTFE surfaces as a function of the test fluid (water, oil, Water 60%+EtOH 40%, and Water 80%+EtOH 20%).

3.4. Potential applications of CO_2 laser treated PTFE surfaces

As demonstrated, CO_2 laser texturing can tailor the wettability of PTFE surfaces in one step, without the need for chemicals or the control of the atmosphere, and in a fast and inexpensive way as low power CO_2 lasers (commonly used in the industry) are used.

In the following, we will describe the potential application of these laser-treated surfaces for self-cleaning purposes. However, the wettability of these laser-textured surfaces can be tailored for different test fluids, as observed; therefore, these surfaces could also be applied, for example, in oil/water separation or in similar applications [43].

3.4.1. Self-cleaning surfaces

Self-cleaning surfaces refer to surfaces that reduce or avoid the surface contamination by dust, organic matter, stains or other surface contaminants [44, 45]. Self-cleaning effect has been observed in superhydrophilic surfaces or superhydrophobic (lotus leaf effect) [46]. In both cases, the cleaning effect is produced by the washing away the contaminants by the action of water propelled by the action of the gravity [46]. In the first case, a thin sheet of water running off a surface and washing away contaminants produces the cleaning effect. In the second case, water droplets rolling off the surface picks up the contaminant particles along their path to produce the cleaning effect.

Figure 9 (see also the Supplementary Video 1) shows the self-cleaning performance of the PFTE surfaces after laser texturing. AISI 316L powder (powder size 63-125 µm, ORIC S.A.S, France) was used as contaminant on the pristine and laser-treated PTFE surfaces. Water droplets were dispensed on the surface, which is tilted ≈15° in all the cases. As observed, water droplets supplied to the pristine PFTE surfaces are adsorbed by the powder, and remain adhered on the impact location. It is required the supply of a large amount of water droplets to the same location to obtain an enough volume able to remove some part of the powder by the action of the gravity; however, part of the slurry produced by the addition of water droplets to the powder remains adhered to the surface. On the contrary, water droplets can freely roll along the laser-textured PFTE samples. The water droplet slides on the surface quite quickly in a very short time (about 150 ms) demonstrating an excellent low adhesive superhydrophobicity property. One water droplet is able to clean a large amount of powder during its travel. Therefore, results showed that these laser-textured PTFE surfaces exhibits an excellent lotus-like self-cleaning effect.

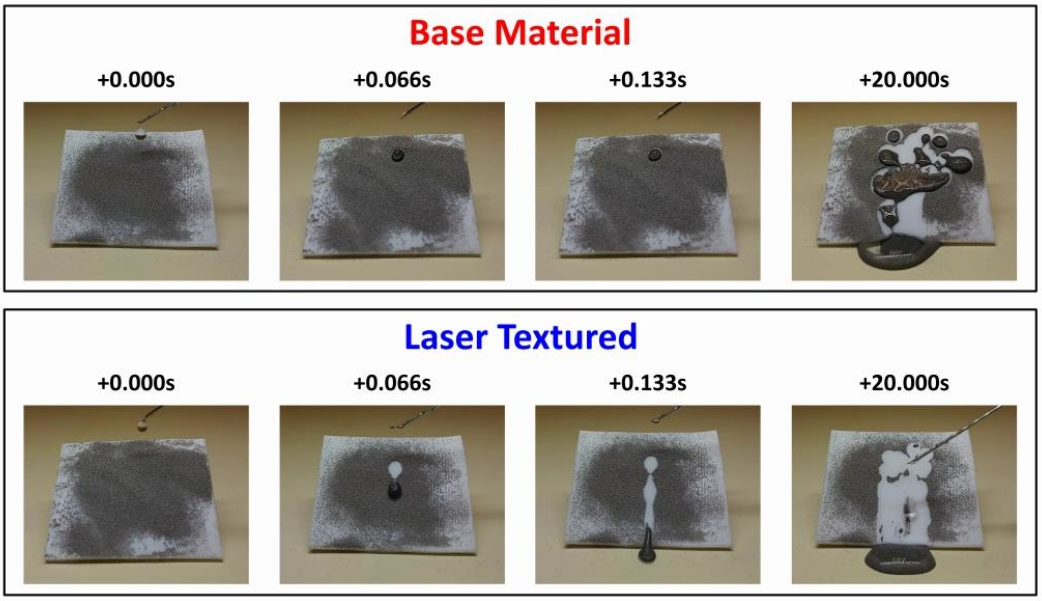

Figure 9. Comparison of the self-cleaning process in a pristine and laser-textured PTFE surface, using AISI 316L powder (powder size 63-125 µm, ORIC S.A.S, France) as contaminant material (see Supplementary Video 1).

To date, research works found in the literature conclude that the self-cleaning properties in superhydrophobic surfaces is severely compromised by corrosion because the surface topography is destroyed [47-49]. In the present case, the self-cleaning effect remains even after being the laser-treated surfaces immersed into acid or alkali solutions as the chemical

composition and nature of the laser-textured surfaces remain intact. The laser textured surfaces remain very stable when contacting with aqueous HNO_3 (pH = 1) and aqueous NaOH (pH = 14) solutions. Optical images of a water droplets with different pH values on the treated areas are shown in Fig. 10a. These droplets exhibit typical spherical shapes on the surface. Furthermore, these laser textured surfaces were immersed into aqueous HNO_3 (pH = 1) NaOH (pH = 14) solutions for 2 h to demonstrate the stability of the treated areas. As observed in Fig. 10b, the water contact angle is not altered by the attack with strong acid or alkali solutions. Therefore, the large chemical resistance of these laser textured areas is demonstrated.

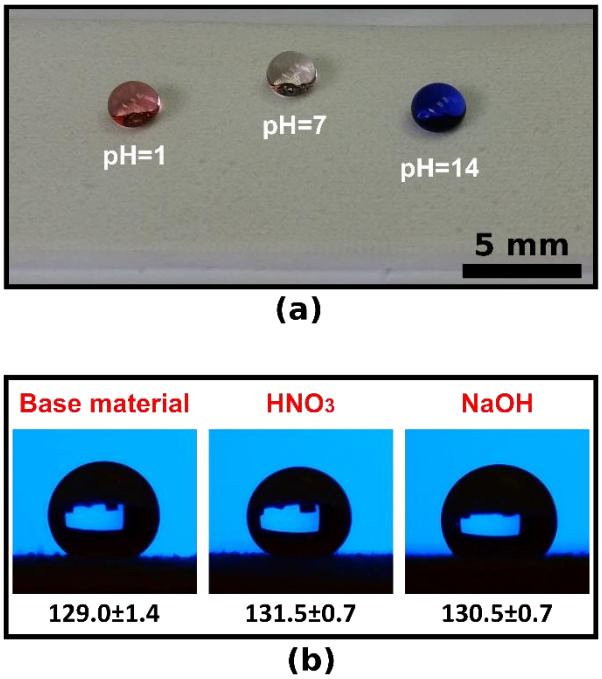

Figure 10. a) Images of different water droplets (pH=1, 7, and 14) on the laser textured surface. b) Contact angles of a water droplet on a laser textured surface after being immersed into a HNO_3 (pH=1) and NaOH (pH=14) solution for 2h.

Most of the superhydrophobic coatings reported in the literature are very fragile when subjected to mechanical forces, and even cannot withstand a slight contact because the hierarchical structure is easily broken when touched [50, 51]. In this sense, the laser-textured PTFE surfaces remain almost unaltered under slight friction conditions. Figure 11 displays the finger-wipe test on a laser-textured PTFE surface [52-54]. After this qualitative test, the wettability of the surface remains unaltered after several friction cycles and the water droplets rolled under the action of the gravity. Scraped surfaces still maintain the spongy-like surface structure after 50 friction cycles, and also the self-cleaning property, as shown in Fig. 11.

Therefore, these surfaces will not be destroyed in environmental conditions where some slight contact with the treated areas is required (e.g. in the application of these treatments in pipes for drag reduction, where a continuous and fast flow could damage the textured surface).

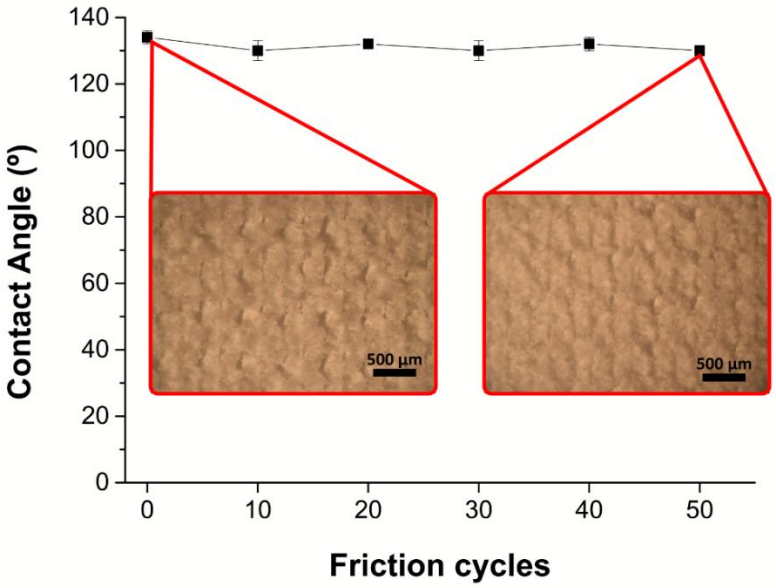

Figure 11. Finger-wipe test on a laser-textured PTFE surface. Wettability remains intact after 50 friction cycles.

4. Conclusions

The current work determines the influence of the laser processing parameters (laser power or irradiance, scanning speed, and spacing between scan lines) on the wetting properties on PTFE surfaces after CO_2 laser texturing. Wetting properties were determined for different test fluids (water, mineral oil, water 60%+ethanol 40% and water 80%+ethanol 20%). In all the cases, the wettability of the laser-treated PTFE surfaces is substantially reduced, especially for water, where superhydrophobic surfaces are produced. This reduction in wettability is associated to the rough surfaces produced during the CO_2 laser texturing. Grooves with protruding filaments are observed after the processing. This spongy-like structure has many voids where air is trapped. These are responsible for the reduction in wettability, as chemical modifications in the treated areas were not detected. Finally, it was showed that these surfaces are resistant to the attach with strong acid or alkali solutions, they remain almost unaltered under slight friction conditions, and are suitable for self-cleaning applications.

Acknowledgments

The authors wish to thank the technical staff from CACTI (University of Vigo) for their help with sample characterization. This work was partially supported by the EU research project Bluehuman (EAPA_151/2016 Interreg Atlantic Area), Government of Spain [RTI2018-095490-J-I00 (MCIU/AEI/FEDER, UE), FPU16/05492], and by Xunta de Galicia (ED431C 2019/23, ED481D 2017/010, ED481B 2016/047-0, POS-A/2013/161). The technical staff from CACTI (University of Vigo) is gratefully acknowledged.

References

[1] S. Lee, K.S. Knaebel, Effects of mechanical and chemical properties on transport in fluoropolymers. I. Transient sorption, Journal of Applied Polymer Science, 64 (1997) 455-476.

[2] S. Lee, K.S. Knaebel, Effects of mechanical and chemical properties on transport in fluoropolymers. II. Permeation, Journal of Applied Polymer Science, 64 (1997) 477-492.

[3] F. Garbassi, M. Morra, E. Occhiello, F. Garbassi, Polymer surfaces: from physics to technology, Wiley Chichester, 1998.

[4] J. Gardiner, Fluoropolymers: Origin, Production, and Industrial and Commercial Applications, Australian Journal of Chemistry, 68 (2015) 13-22.

[5] J. Reichert, S. Brückner, H. Bartelt, K.D. Jandt, Tuning Cell Adhesion on PTFE Surfaces by Laser Induced Microstructures, Advanced Engineering Materials, 9 (2007) 1104-1113.

[6] D.J. Wilson, R.L. Williams, R.C. Pond, Plasma modification of PTFE surfaces. Part I: Surfaces immediately following plasma treatment, Surface and Interface Analysis, 31 (2001) 385-396.

[7] J. Yong, Y. Fang, F. Chen, J. Huo, Q. Yang, H. Bian, G. Du, X. Hou, Femtosecond laser ablated durable superhydrophobic PTFE films with micro-through-holes for oil/water separation: Separating oil from water and corrosive solutions, Applied Surface Science, 389 (2016) 1148-1155.

[8] Z. Qin, J. Ai, Q. Du, J. Liu, X. Zeng, Superhydrophobic polytetrafluoroethylene surfaces with accurately and continuously tunable water adhesion fabricated by picosecond laser direct ablation, Materials & Design, 173 (2019) 107782.

[9] Y.L. Zhan, M. Ruan, W. Li, H. Li, L.Y. Hu, F.M. Ma, Z.L. Yu, W. Feng, Fabrication of anisotropic PTFE superhydrophobic surfaces using laser microprocessing and their self-cleaning and

anti-icing behavior, Colloids and Surfaces A: Physicochemical and Engineering Aspects, 535 (2017) 8-15.

[10] J. Ryu, K. Kim, J. Park, B.G. Hwang, Y. Ko, H. Kim, J. Han, E. Seo, Y. Park, S.J. Lee, Nearly Perfect Durable Superhydrophobic Surfaces Fabricated by a Simple One-Step Plasma Treatment, Scientific Reports, 7 (2017) 1981.

[11] L.R.J. Scarratt, B.S. Hoatson, E.S. Wood, B.S. Hawkett, C. Neto, Durable Superhydrophobic Surfaces via Spontaneous Wrinkling of Teflon AF, ACS Applied Materials & Interfaces, 8 (2016) 6743-6750.

[12] D. Song, R.J. Daniello, J.P. Rothstein, Drag reduction using superhydrophobic sanded Teflon surfaces, Experiments in Fluids, 55 (2014) 1783.

[13] M. Toma, G. Loget, R.M. Corn, Flexible Teflon Nanocone Array Surfaces with Tunable Superhydrophobicity for Self-Cleaning and Aqueous Droplet Patterning, ACS Applied Materials & Interfaces, 6 (2014) 11110-11117.

[14] F. Liang, J. Lehr, L. Danielczak, R. Leask, A.-M. Kietzig, Robust non-wetting PTFE surfaces by femtosecond laser machining, International journal of molecular sciences, 15 (2014) 13681-13696.

[15] F.J. Wang, S. Lei, J.F. Ou, M.S. Xue, W. Li, Superhydrophobic surfaces with excellent mechanical durability and easy repairability, Applied Surface Science, 276 (2013) 397-400.

[16] J. Heitz, J.D. Pedarnig, D. Bäuerle, G. Petzow, Excimer-laser ablation and micro-patterning of ceramic Si3N4, Applied Physics A, 65 (1997) 259-261.

[17] A. Riveiro, R. Soto, R. Comesaña, M. Boutinguiza, J. del Val, F. Quintero, F. Lusquiños, J. Pou, Laser surface modification of PEEK, Applied Surface Science, 258 (2012) 9437-9442.

[18] A. Riveiro, A.L.B. Maçon, J. del Val, R. Comesaña, J. Pou, Laser Surface Texturing of Polymers for Biomedical Applications, Frontiers in Physics, 6 (2018).

[19] P. Pou, J. del Val, A. Riveiro, R. Comesaña, F. Arias-González, F. Lusquiños, M. Bountinguiza, F. Quintero, J. Pou, Laser texturing of stainless steel under different processing atmospheres: From superhydrophilic to superhydrophobic surfaces, Applied Surface Science, 475 (2019) 896-905.

[20] A. Riveiro, R. Soto, J. Del Val, R. Comesaña, M. Boutinguiza, F. Quintero, F. Lusquiños, J. Pou, Laser surface modification of ultra-high-molecular-weight polyethylene (UHMWPE) for biomedical applications, Applied Surface Science, 302 (2014) 236-242.

[21] A. Riveiro, R. Soto, J. Del Val, R. Comesaña, M. Boutinguiza, F. Quintero, F. Lusquiños, J. Pou, Texturing of polypropylene (PP) with nanosecond lasers, Applied Surface Science, 374 (2016) 379-386.

[22] Z.M. Huang, M. Zhou, C. Li, J. Li, B. Wu, Femtosecond laser on the surface of PTFE, Gongneng Cailiao/Journal of Functional Materials, 41 (2010) 2163-2165.

[23] A.M. Kietzig, J. Lehr, L. Matus, F. Liang, Laser-induced patterns on metals and polymers for biomimetic surface engineering, in: Proc. SPIE 8967, Laser Applications in Microelectronic and Optoelectronic Manufacturing (LAMOM) XIX, San Francisco, CA, United States, 2014.

[24] F. Liang, J. Lehr, L. Danielczak, R. Leask, A.M. Kietzig, Robust non-wetting PTFE surfaces by femtosecond laser machining, International Journal of Molecular Sciences, 15 (2014) 13681-13696.

[25] W. Li, Q. Yang, F. Chen, J. Yong, Y. Fang, J. Huo, Femtosecond laser ablated durable superhydrophobic PTFE sheet for oil/water separation, in, 2017.

[26] S.F. Toosi, S. Moradi, S. Kamal, S.G. Hatzikiriakos, Superhydrophobic laser ablated PTFE substrates, Applied Surface Science, 349 (2015) 715-723.

[27] W. Fan, J. Qian, F. Bai, Y. Li, C. Wang, Q.Z. Zhao, A facile method to fabricate superamphiphobic polytetrafluoroethylene surface by femtosecond laser pulses, Chemical Physics Letters, 644 (2016) 261-266.

[28] J.H. Yoo, H.J. Kwon, D. Paeng, J. Yeo, S. Elhadj, C.P. Grigoropoulos, Facile fabrication of a superhydrophobic cage by laser direct writing for site-specific colloidal self-assembled photonic crystal, Nanotechnology, 27 (2016).

[29] K. Gotoh, Y. Nakata, M. Tagawa, M. Tagawa, Wettability of ultraviolet excimer-exposed PE, PI and PTFE films determined by the contact angle measurements, Colloids and Surfaces A: Physicochemical and Engineering Aspects, 224 (2003) 165-173.

[30] B. Hopp, Z. Geretovszky, I. Bertóti, I.W. Boyd, Comparative tensile strength study of the adhesion improvement of PTFE by UV photon assisted surface processing, 186 (2002) 80-84.

[31] S. Inazaki, T. Oie, H. Takaoka, Surface modification of polytetrafluoroethylene with ArF excimer laser irradiation, Journal of Photopolymer Science and Technology, 7 (1994) 389-396.

[32] Z. Qin, J. Ai, Q. Du, J. Liu, X. Zeng, Superhydrophobic polytetrafluoroethylene surfaces with accurately and continuously tunable water adhesion fabricated by picosecond laser direct ablation, Materials and Design, 173 (2019).

[33] A. Žemaitis, J. Mikšys, M. Gaidys, P. Gečys, M. Gedvilas, High-efficiency laser fabrication of drag reducing riblet surfaces on pre-heated Teflon, Materials Research Express, 6 (2019) 065309.

[34] D.G. Waugh, J. Lawrence, P. Shukla, Modulating the wettability characteristics and bioactivity of polymeric materials using laser surface treatment, Journal of Laser Applications, 28 (2016).

[35] V. Tarasenko, V. Orlovskii, A. Fedenev, M. Shulepov, Temperature dependence of Teflon transmission factor under ТЕА-СО2 laser irradiation, SPIE, 2004.

[36] E.M. Tolstopyatov, L.F. Ivanov, P.N. Grakovich, A.M. Krasovsky, Destruction of polytetrafluoroethylene under the action of carbon dioxide laser radiation at low pressure, in: Proceedings of SPIE - The International Society for Optical Engineering, International Society for Optics and Photonics, 1998, pp. 1010-1017.

[37] X. Chen, H.-X. Wang, A calculation model for the evaporation recoil pressure in laser material processing, Journal of Physics D: Applied Physics, 34 (2001) 2637-2642.

[38] M. Goessi, T. Tervoort, P. Smith, Melt-spun poly(tetrafluoroethylene) fibers, Journal of Materials Science, 42 (2007) 7983-7990.

[39] E.M. Tolstopyatov, L.F. Ivanov, P.N. Grakovich, A.M. Krasovsky, Destruction of polytetrafluoroethylene under the action of carbon dioxide laser radiation at low pressure, in: Proceedings of SPIE, Volume 3343, High-Power Laser Ablation, SPIE, Santa Fe, NM, United States, 1998, pp. 1010-1017.

[40] M.R. Jung, F.D. Horgen, S.V. Orski, V. Rodriguez C, K.L. Beers, G.H. Balazs, T.T. Jones, T.M. Work, K.C. Brignac, S.-J. Royer, K.D. Hyrenbach, B.A. Jensen, J.M. Lynch, Validation of ATR FT-IR to identify polymers of plastic marine debris, including those ingested by marine organisms, Marine Pollution Bulletin, 127 (2018) 704-716.

[41] A.J.B. Milne, A. Amirfazli, The Cassie equation: How it is meant to be used, Advances in Colloid and Interface Science, 170 (2012) 48-55.

[42] Y. Xiu, L. Zhu, D.W. Hess, C.P. Wong, Relationship between Work of Adhesion and Contact Angle Hysteresis on Superhydrophobic Surfaces, The Journal of Physical Chemistry C, 112 (2008) 11403-11407.

[43] G. Ren, Y. Song, X. Li, Y. Zhou, Z. Zhang, X. Zhu, A superhydrophobic copper mesh as an advanced platform for oil-water separation, Applied Surface Science, 428 (2018) 520-525.

[44] R. Blossey, Self-cleaning surfaces — virtual realities, Nature Materials, 2 (2003) 301-306.

[45] K. Liu, L. Jiang, Bio-Inspired Self-Cleaning Surfaces, Annual Review of Materials Research, 42 (2012) 231-263.

[46] S. Nishimoto, B. Bhushan, Bioinspired self-cleaning surfaces with superhydrophobicity, superoleophobicity, and superhydrophilicity, RSC Advances, 3 (2013) 671-690.

[47] M.J. Nine, M.A. Cole, L. Johnson, D.N. Tran, D. Losic, Robust superhydrophobic graphene-based composite coatings with self-cleaning and corrosion barrier properties, ACS applied materials & interfaces, 7 (2015) 28482-28493.

[48] S.S. Latthe, P. Sudhagar, A. Devadoss, A.M. Kumar, S. Liu, C. Terashima, K. Nakata, A. Fujishima, A mechanically bendable superhydrophobic steel surface with self-cleaning and corrosion-resistant properties, Journal of Materials Chemistry A, 3 (2015) 14263-14271.

[49] C. Lv, H. Wang, Z. Liu, W. Zhang, C. Wang, R. Tao, M. Li, Y. Zhu, A sturdy self-cleaning and anti-corrosion superhydrophobic coating assembled by amino silicon oil modifying potassium titanate whisker-silica particles, Applied Surface Science, 435 (2018) 903-913.

[50] T. Verho, C. Bower, P. Andrew, S. Franssila, O. Ikkala, R.H.A. Ras, Mechanically Durable Superhydrophobic Surfaces, Advanced Materials, 23 (2011) 673-678.

[51] A. Milionis, E. Loth, I.S. Bayer, Recent advances in the mechanical durability of superhydrophobic materials, Advances in Colloid and Interface Science, 229 (2016) 57-79.

[52] J. Huang, S. Wang, S. Lyu, Facile Preparation of a Robust and Durable Superhydrophobic Coating Using Biodegradable Lignin-Coated Cellulose Nanocrystal Particles, Materials, 10 (2017) 1080.

[53] K. Tu, X. Wang, L. Kong, H. Chang, J. Liu, Fabrication of robust, damage-tolerant superhydrophobic coatings on naturally micro-grooved wood surfaces, RSC Advances, 6 (2016) 701-707.

[54] M. Yu, Q. Wang, W. Yang, Y. Xu, M. Zhang, Q. Deng, G. Liu, Facile Fabrication of Magnetic, Durable and Superhydrophobic Cotton for Efficient Oil/Water Separation, Polymers, 11 (2019) 442.